Influence of process damping on the regenerative instability of guided metal circular sawing

Sunny Singhania, Mohit Law*

Indian Institute of Technology Kanpur, Kanpur, India

Presented in International Conference on Precision, Micro, Meso and Nano Engineering (COPEN - 12: 2022)
December 8 - 10, 2022 IIT Kanpur, India

ABSTRACT

Circular saws are thin and hence they vibrate during cutting. Vibrations get imprinted on the side walls of the part being cut, with each tooth leaving its own imprint. When there is a phase shift of vibrations between two successive teeth, regenerative instabilities can occur. However, since the flank face of the tooth also rubs the vibration marks on the side wall, there can also be process-induced damping. Such damping is known to improve the stability of low speed cutting processes. Since metal circular sawing is a low-speed process, it is the aim of this paper to characterize the role of process damping, if any, on regenerative instabilities using an analytical model. The saw is modelled as an annular disc constrained by springs representing guides. The Muller method with deflation is used to solve the governing equations of motion. Model-based analysis suggests that process damping indeed plays a stabilizing role.

KEYWORDS

Regenerative Instabilities,
Damping,
Vibrations,
Circular Sawing.

1. Introduction

A rotating saw is fed into a workpiece to cut parts to the required lengths in circular sawing. Saws are usually kept thin to minimise kerf losses. Due to their thinness, they vibrate and are susceptible to critical speed-related instabilities and process induced regenerative instabilities. These instabilities are detrimental to the saw, the part, and the machine. These instabilities occur even when the saw's out-of-plane motion is constrained by guides (Hutton et al., 1986; Lehmann & Hutton, 1988; Singhania et al., 2019; Singhania et al., 2022; Tian & Hutton, 1999; Tian & Hutton, 2001; Singhania & Law, 2021). Critical speeds occur when the saw's rotational speed matches one of the many backward travelling wave's natural frequency as it tends to become stationary (Hutton et al., 1986). Regenerative instabilities occur when there is an unfavourable phase shift of vibration marks left on the side walls of the part being cut between two successive teeth (Tian & Hutton, 2001; Singhania & Law, 2021). For metal sawing, regenerative instabilities occur at speeds lower than critical (Singhania & Law, 2021). As such, this paper is only concerned with instabilities of the regenerative kind.

Regenerative instabilities in sawing are governed only by the lateral regenerative forces (Tian & Hutton, 2001; Singhania & Law, 2021), and not by the in-plane radial and/or tangential forces as they are in other milling processes (Altintas & Budak, 1995). Speed-regions of instabilities are further influenced by changing engagement conditions and by changing number of teeth in cut as the saw enters and exits the part it is cutting. Moreover, the characteristics of the workpiece material being cut also significantly influence such instabilities. This behaviour has been characterized for saws with and without guides (Tian & Hutton, 2001; Singhania & Law, 2021).

Regenerative instabilities are also influenced by the rubbing action of the flank face interacting with the vibration marks left on the surface being cut. This interaction is described as process damping (Wallace & Andrew, 1965; Eynian, 2010; Gurdal et al., 2016). This process-induced interaction is governed by the cutting tooth's geometry, by the cutting speed, and by the frequency and amplitude of vibrations left on the surface. Process damping has been reported to improve the stability margin in turning and milling

*Corresponding author E-mail: mlaw@iitk.ac.in

https://doi.org/10.58368/MTT.22.4.2023.20-25

processes damping (Wallace & Andrew, 1965; Eynian, 2010; Gurdal et al., 2016), especially at low speeds.

Since metal circular sawing is a low-speed process, and since the role of process damping in sawing has not been investigated and/or reported yet, it is the explicit aim of this paper to characterize the role of process damping, if any, on regenerative instabilities. This is also the primary new technical advancement of this paper to the state-of-the-art.

Since instabilities are detrimental, and since these are governed by the dynamics of the saw, by the number of teeth, by the geometry of those teeth, by the workpiece material being cut, and by the number, location, and size of guides, the experimental route to characterize the role of process damping is prohibitive. This paper will hence present systematic model-based analysis. The analytical model for the saw is a thin circular disc laterally restricted by guides modelled as point springs is presented in Section 2 of this paper. The model builds on our earlier reports (Singhania et al., 2019; Singhania et al., 2022; Singhania & Law, 2021), and incorporates the influence of lateral regenerative forces together with the process damping forces. The Muller method with deflation (Mathews, 1992) is used to solve the resulting governing equations of motion. Section 3 discusses the influence of process damping. Main conclusions follow.

2. Model for the Guided Saw Subjected to Regenerative and Process Damping Forces

The saw is modelled as an annular disc rotating counterclockwise with an angular velocity Ω with a clamped inner radius b, free outer radius a, and thickness h. As shown in Fig. 1, the saw is cutting a solid bar. The instantaneous entry angle of the saw entering the bar is γ_{st}. The exit angle is γ_{ex}. These angles change as the cut progresses. The saw is laterally constrained by distributed guides positioned symmetrically with respect to the cutting zone. These guides are assumed to be fixed independently on the machine frame. Usually, these guides are lubricated. Though the stiffness of these distributed guides is also distributed, for analysis herein we model it as a lumped point spring, characteristics of which are a function of the fluid's stiffness and the clearance. These springs are assumed placed at a radial location $\boldsymbol{r}_m$ and an angular location γ_m at the geometrical centre of the guide pad. Other modelling assumptions remain as those that this report builds on

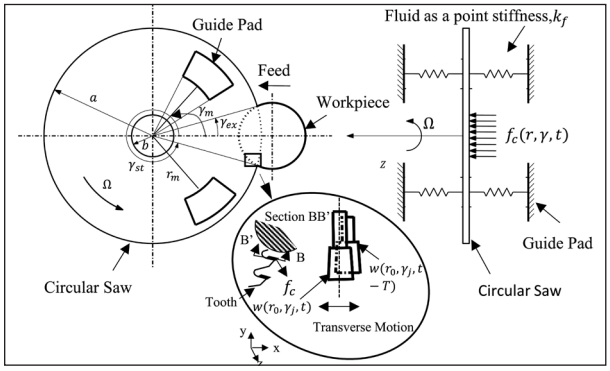

Fig. 1. Schematic showing lateral regenerative cutting forces on a circular saw constrained with guides modelled as point springs.

(Singhania et al., 2019; Singhania et al., 2022; Singhania & Law, 2021).

We additionally assume that the only cutting forces of interest are the lateral regenerative cutting forces *($f_c(t)$)* and hence ignore any in-plane radial and tangential forces. As shown in the section BB' in the inset in Fig. 1, the regenerative effect is associated with an extra lateral cutting area between two successive teeth associated with the transverse response $w(\boldsymbol{r}_o, \gamma_j, t)$, of the current tooth (the jth tooth) and the transverse response $w(\boldsymbol{r}_o, \gamma_j, t\text{-}T)$, of the preceding tooth (the (j-1)th tooth) at a given location $(\boldsymbol{r}_o, \gamma_j)$ of the workpiece (Tian & Hutton, 2001; Singhania & Law, 2021). $T=2\pi/\Omega N_t$ is the tooth passing period, i.e., the interval between two consecutive teeth coming into cut. In addition to these regenerative forces, there are also forces due to the guide modelled as a spring, and additional forces due to the process damping phenomena.

With these forces acting on the system the governing differential equation of the rotating saw in terms of its transverse displacement, $\tilde{w}(r,\gamma,t)$ subjected to all three forces, $f(r,\gamma,t)$ in the stationary frame of reference can be shown to be:

$$D\nabla^4\tilde{w} + D^*\nabla^4\left(\tilde{w}_{,t} + \Omega\tilde{w}_{,\gamma}\right) + \rho h\left\{\tilde{w}_{,tt} + 2\Omega\tilde{w}_{,t\gamma} + \Omega^2\tilde{w}_{,\gamma\gamma}\right\} - \frac{h}{r}\left\{\left(r\sigma_r\tilde{w}_{,r}\right)_{,r} + \left(\frac{\sigma_\gamma}{r}\tilde{w}_{,\gamma}\right)_{,\gamma}\right\} = f(r,\gamma,t) \quad \text{.....(1)}$$

wherein the comma-subscript notation signifies partial differentiation, ρ is the mass density, h is the saw's thickness, $D = \frac{Eh^3}{12(1-\nu^2)}$ is the flexural rigidity, wherein E is the Young's modulus, ν is the Poisson's ratio, $D*=\eta D$ is the internal damping in the saw, wherein η is the Kelvin-Voigt damping parameter,

∇^4 is the bi-harmonic operator, and σr, $\sigma\gamma$, are the in-plane stresses due to rotation.

$f(r,\gamma,t)$ in Eq. (1) is the point force on the saw that is comprised of forces due to the lubricated guides $f_g(r,\gamma,t)$, the lateral regenerative cutting forces $f_c(r,\gamma,t)$, and the process damping forces $f_p(r,\gamma,t)$. Of these, the guide forces take the form of:

$$f_g(r,\gamma,t) = \sum_{j=1}^{J}\left(\frac{1}{r}\right)\left[\left\{-k_{f_j}\tilde{w}(r,\gamma,t)\right\}\left\{\delta\left(\gamma-\gamma_{\mathrm{m_j}}\right)\right\}\left\{\delta\left(r-r_{\mathrm{m_j}}\right)\right\}\right] \quad \text{.....(2)}$$

wherein k_{fj} is the stiffness between the j^{th} guide pad pair and the saw, respectively, which is modelled as: $k_{f_j}=\frac{E_{f_j}}{h_{f_j}}$, wherein E_{fj} and h_{fj} are the stiffness constant and the clearance between the j^{th} guide pad pair and the saw, respectively. J in Eq. (2) is the total number of point springs, and $\delta(.)$ is the Dirac delta function.

The regenerative forces take the form of:

$$f_c(r,\gamma,t) = -\sum_{j=1}^{N_t}\left(\frac{1}{r}\right)K_r[\tilde{w}(r,\gamma,t)-\tilde{w}(r,\gamma,t-T)]\delta(r-r_0)\delta(\gamma-\gamma_j)\,g(\gamma_j) \quad \text{.....(3)}$$

wherein N_t is the total number of teeth in cut, and K_r is an empirically estimated cutting force coefficient that is usually a function of the saw tooth's geometry, the workpiece material being cut, and the cutting conditions (Altintas & Budak, 1995). $g(\gamma_j)$ is a screening function to determine if the tooth is in cut or not, i.e., $g(\gamma_j)$= 1, when $\gamma_{st}<\gamma_j<\gamma_{ex}$, and $g(\gamma_j)=0$ otherwise. The instantaneous tooth position γ_j is given by: $\gamma_j=\gamma_{st}+\Omega t+(j-1)\gamma_p$,($\gamma_i=\gamma_{st}$ when $t=0$;γ_p is the angular pitch).

The process damping forces take the form of:

$$f_p(r,\gamma,t) = -\sum_{j=1}^{N_t}\left(\frac{1}{r}\right)\left\{C_i\left(\frac{S}{\Omega r}\right)\tilde{w}_{,t}(r,\gamma,t)\right\}\delta(r-r_0)\delta(\gamma-\gamma_j)g(\gamma_j) \quad \text{.....(4)}$$

wherein C_i is also an process damping coefficient that is empirically determined and depends on the material being cut, the cutting speed, the saw tooth's geometry, potential wear of that tool, and vibration frequency and amplitudes (Wallace & Andrew, 1965; Eynian, 2010; Gurdal et al., 2016). $\tilde{w}_{,t}(r,\gamma,t)$ within Eq. (4) is the vibrational velocity of saw in the transverse direction, and S is width of cut at minor cutting edge as shown in the schematic in Fig.2.

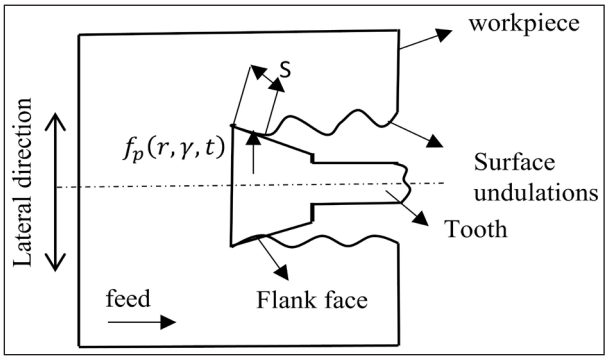

Fig. 2. Schematic of process damping force acting on a tooth along the lateral direction.

The governing equation is approximately solved by assuming a solution of the form (Tian & Hutton, 2001):

$$\tilde{w}(r_0,\gamma_j,t) = \sum_{m=0}^{M}\sum_{n=0}^{N}\{C_{mn}(t)\,cos(n\gamma_j)+S_{mn}(t)\,sin(n\gamma_j)\}R_{mn}(r_0) \quad \text{.....(5)}$$

wherein M and N represent the number of nodal circles and nodal diameters, respectively, r_0 is the radial location of the clamped saw's outer free edge and $R_{mn}(r)$ satisfies the boundary conditions of the saw being clamped at its inner section and free at its periphery, and $C_{mn}(t)$ and $S_{mn}(t)$ are variable coefficients.

Substituting Eq. (2) to Eq. (5) in the governing equation i.e., Eq. (1) and applying the Galerkin's procedure results in an equation of motion of the form:

$$[\boldsymbol{M}]\{\ddot{\boldsymbol{x}}\}+[\boldsymbol{G}]\{\dot{\boldsymbol{x}}\}+[\boldsymbol{K}]\{\boldsymbol{x}\}+(1-e^{-TD})[\boldsymbol{A}(t)]\{\boldsymbol{x}\}=\{\boldsymbol{0}\} \quad \text{.....(6)}$$

wherein $e^{-TD}\{\boldsymbol{x}(t)\}=\{\boldsymbol{x}(t-T)\}$, and $\{\boldsymbol{x}(t)\}$ is an array of $\{C_{mn}(t)\ S_{mn}(t)\}^T$, and $[M]$, $[G]$, and $[K]$ are mass, gyroscopic and/or damping, and stiffness matrices, respectively. $[A(t)]$ within Eq. (6) is a time periodic varying matrix associated with the lateral regenerative cutting forces.

To solve the stability problem for the time-varying periodic system of differential equations, the basic Fourier series method is used. With periodic coefficients, the solution to Eq. (6) can be assumed of as a Fourier series:

$$\{\boldsymbol{x}(t)\}=\left[\frac{\{\boldsymbol{b_0}\}}{2}+\sum_{k=1}^{\infty}(\{\boldsymbol{a_k}\}\sin(kwt))+\{\boldsymbol{b_k}\}\cos(kwt)\right]e^{\lambda t} \quad \text{.....(7)}$$

wherein $\{b_0\}$, $\{\boldsymbol{a_k}\}$ and $\{b_k\}$ are time-invariant coefficient vectors, and λ is the characteristic

variable of the system. Since $[A(t)]$ is also periodic, as proposed in (Altintas & Budak, 1995) for the case of a regenerative model for milling processes, it can be expressed in Fourier series form in this case as well:

$$[\boldsymbol{A}(t)] = \left[\frac{[\boldsymbol{B_0}]}{2} + \sum_{k=1}^{\infty}([\boldsymbol{A_k}]\sin(kwt)) + [\boldsymbol{B_k}]\cos(kwt)\right] \quad \text{.....(8)}$$

wherein $[B_0]$,$[A_k]$ and $[B_k]$ are defined as in (Tian & Hutton, 2001; Singhania & Law, 2021).

Substituting Eq. (7) and Eq. (8) into Eq. (6) and using the zeroth order approximation results in:

$$\left(\lambda^2[\boldsymbol{M}] + \lambda[\boldsymbol{G}] + [\boldsymbol{K}] + \left(1 - e^{-T\lambda}\right)\left[\frac{\boldsymbol{B_0}}{2}\right]\right)\{\boldsymbol{b_0}\} = \{\boldsymbol{0}\}. \quad \text{.....(9)}$$

The resulting eigenvalues are complex valued, i.e., wherein the imaginary part corresponds to the natural frequency of the system and real part represent the growth and/or decay. Since Eq. (9) is a complex nonlinear equation, hence, Muller's optimization algorithm (Mathews, 1992) with deflation gives the system's eigenvalues for every speed of interest.

Having discussed the governing equations of motion and methods to solve them, we next present model-based analysis to characterize the role of process damping on the regenerative instabilities of a metal circular sawing process.

3. Numerical Analysis and Discussion

This section discusses how the introduction of point guides and process-induced damping affects instability. For instantaneous cutting under a constant engagement condition, the instabilities of point guides and unguided saws cutting a specified material with a constant cutting force coefficient are compared in Section 3.1. This is followed by a discussion in Section 3.2 on how process damping influences instabilities for a guided saw configuration.

All analyses reported herein are for a multimode case, i.e., (M,N) = (0,4), with a circular saw with the following material and geometry: ρ= 7850 Kg/m^3, E=210 GPa, ν= 0.3, a= 142.5 mm, b=42.5 mm, h=2 mm, h_f=0.15 mm,η=10^{-6} sec, N_t= 60. We assume that the saw is constrained with two oil-lubricated guides. This is in line with industrial praxis. These oil-lubricated guides are modelled as point springs, with their stiffness parameters taken from (Singhania et al., 2022). The guides are assumed placed at a radial location of r_m=125mm, and with an angular orientation of two guides, γ_{m1}=25^0 and γ_{m2}=335^0 as shown in Fig. 1. Moreover, for analysis herein, we assume the saw is cutting a bar of 76 mm diameter with an instantaneous entry angle of γ_{st}=343^0, and an exit angle of γ_{ex} =17^0, measured along the counterclockwise direction. Since influence of changing engagements, albeit without process damping, have already been discussed in (Singhania & Law, 2021), results herein are limited to cutting with only one engagement condition.

3.1. Regenerative instabilities of the guided circular saw

We first compare the stability of a saw that is constrained by point guides to one that is not. We presently ignore the role of process damping and discuss its contribution separately in Section 3.2. Regenerative forces are assumed acting on the saw that is guided and not. We assume that the material being cut has a cutting force coefficient of K_r = 1000 N/m. Fig. shows the real and imaginary parts of the eigenvalues for this system. These characterize the dynamics and the stability. Results are shown changing with the tooth passing frequency, and not speed. However, since we assume 60 teeth on the saw, the tooth passing frequency is the same as the rotational speed in rpm. Since metal sawing is a low-speed operation, results in Fig. 3 are limited to the low tooth passing frequency (speed) range of interest.

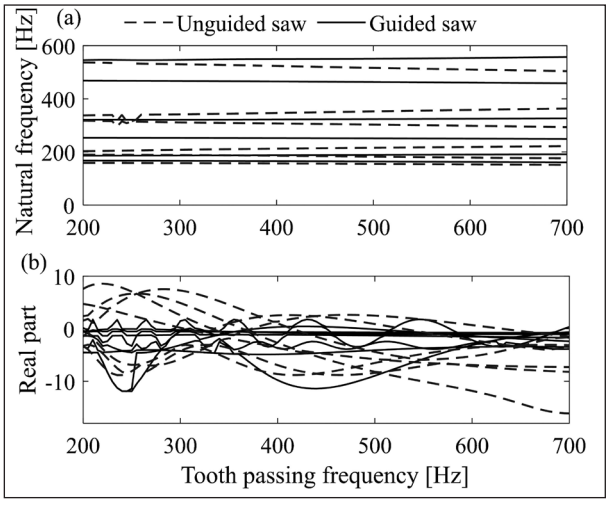

Fig. 3. Comparison of frequency-speed characteristics of saw with and without a guide
(a) Natural frequency, (b) Real part of the eigenvalue.

As is evident from Fig. 3, the real and imaginary parts of the eigenvalues for the guided saw are different than the case of the saw with no guides. Hence, guides clearly play a role in the frequency-speed characteristics. Guides stiffen the response, and as such the natural frequencies (see imaginary part in Fig. 3(a)) are higher than the unguided case. The slopes of the backward waves are also less steep for the guided case, suggesting that the critical speeds occur at higher speeds for a saw that is guided as opposed to a saw that is not. However, the critical speed occurs at speeds beyond the range of interest. Within the low-speed range of interest, it is the real part of the eigenvalue that governs stability of the system, and not critical speeds.

The real parts, as is evident from Fig. 3(b), for the unguided saw are positive over the full speed range of interest. Since the real part being positive suggests that the response grows unbounded, it suggests instability. Different modes become unstable at different speed regions. However, as is also evident from Fig. 3(b), guides play a stabilizing role. Though the real part is not negative throughout the speed region of interest, there are several speed regimes where for the unguided saw, the system was unstable, but for the guided saw, the system is stable. Guides also have a role in reducing the severity of the growth. These results suggest that by tuning the stiffness of the guide along with its size and location relative to the cutting zone, it might be possible to find pockets of stability within which sawing can be done.

3.2. Regenerative instabilities of the guided circular saw with process damping

Results herein show how instabilities are influenced by process damping for a guided saw. Results in Fig. 4 are limited to showing only the real part of the eigenvalues since those are the ones limiting stability and not the imaginary parts which relate to the critical speed, which even with the inclusion of process damping occurs at speeds higher than the tooth passing frequency (speed) of interest. Results in Fig. 4 are generated assuming that K_r = 1000 N/m, and that the process damping coefficient, C_i =10000 N/m, and that the width of the flank face in contact is $S = 0.15$ mm.

With the inclusion of process damping together with regenerative effects in the analysis, the real part becomes negative – see Fig. 4. This confirms that even in sawing, like other machining processes, process damping can stabilize the process at low speeds. And, since metal sawing is inherently a low-speed operation, and since contact of the worn flank face with the vibration marks left on the side walls of the surface being generated are also inevitable, process-induced damping can play a beneficial role.

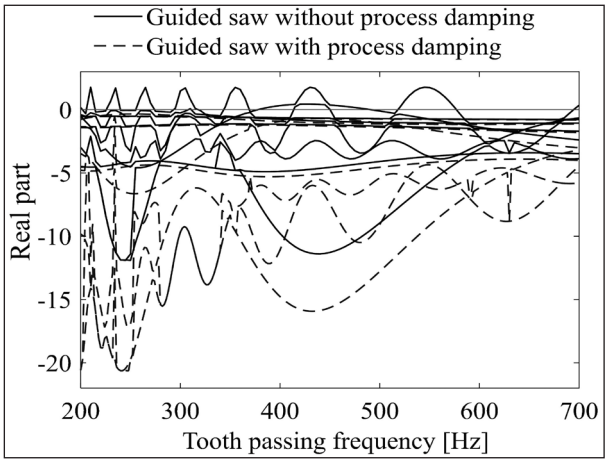

Fig. 4. Comparison of (a) Natural frequency, (b) Real part of the eigenvalue of guided saw with and without process damping.

4. Conclusion

This paper, for the first time, characterized the role of process damping together with regenerative forces on the stability of guided metal circular sawing processes. Model-based analysis revealed that process-induced damping significantly reduces the intensity of unstable vibrations and helps in stabilizing the guided saws. While further research is needed to experimentally validate the model-based observations, our results can still be used to guide the design of stable guided metal sawing processes for industrial applications. For instance, since process damping is a function of the saw tooth's geometry, proposed models can characterize how a change in tooth geometry can help stabilize an otherwise unstable process.

Acknowledgements

This research was supported by the Government of India's Science and Engineering Research Board's Early Career Research Award – SERB/ ECR/2016/000619.

References

Altintas, Y., & Budak, E. (1995). Analytical prediction of stability lobes in milling. *CIRP annals. 44*(1), 357-62. https://doi.org/10.1016/S0007-8506 (07)62342-7

Eynian, M. (2010). Chatter stability of turning and milling with process damping. Ph.D Thesis, University of British Columbia, Canada.

Gurdal, O., Erdum, O., & Sims, N.D. (2016). Analysis of process damping in milling. *Procedia CIRP, 55*, 152-157. https://doi.org/10.1016/j.procir.2016.09.012

Hutton, S. G., Chonan, S., & Lehmann, B. F. (1986). Dynamic response of a guided circular saw. *Journal of Sound and Vibration, 112*(3), 527-539. https://doi.org/10.1016/S0022-460X(87)80116-5

Lehmann, B. F., & Hutton, S. G. (1988). Self-excitation in guided circular saws. *Journal of Vibration and Acoustics, 110*(3), 338-344. https://doi.org/10.1115/1.3269522

Mathews, J. H. (1992). *Numerical methods for mathematics, science and engineering.* Englewood Cliff, Inc. second edition NJ: Prentice-Hall.

Singhania, S., Kumar, P., Gupta, S.K., & Law, M. (2019). Influence of guides on critical speeds of circular saws. *Advances in Computational Methods in Manufacturing*, Springer, 519-530 edited by R. Narayanan., S. Joshi., & U. Dixit. IIT Guwahati. https://doi.org/10.1007/978-981-32-9072-3_45

Singhania, S., Singh, A., & Law, M. (2022). Dynamics and stability of metal cutting circular saws with distributed and lubricated guides. *Journal of Vibration Engineering & Technologies,* 1-13. https://doi.org/10.1007/s42417-022-00544-6

Singhania, S., & Law, M. (2021). Regenerative instabilities of spring-guided circular saws. *9th CIRP Conference on High Performance Cutting, 101,* 142-145. edited by E. Ozturk., D. Curtis., & H. Ghadbeigi. https://doi.org/10.1016/j.procir.2021.02.017

Tian, J. F., & Hutton, S. G. (1999). Self-excited vibration in flexible rotating disks subjected to various transverse interactive forces: A general approach. *ASME Journal of Applied Mechanics,* 800-805. https://doi.org/10.1115/1.2791758

Tian, J. F., & Hutton, S.G. (2001). Cutting-induced vibration in circular saws. *Journal of Sound and Vibration, 242*(5), 907-922. https://doi.org/10.1006/jsvi.2000.3397

Wallace, P. W., & Andrew, C. (1965). Machining Forces: Some Effects of Tool Vibration. *Journal of Mechanical Engineering Science, 7*(2), 152-62. https://doi.org/10.1243/jmes_jour_1965_007_023_02

Sunny Singhania is a Ph.D student at the Department of Mechanical Engineering at the Indian Institute of Technology Kanpur, India. He received his MTech from Indian Institute of Technology BHU Varanasi, India. His research interests centre on understanding the dynamics and stability of circular saw during idling and cutting condition.
(E-mail: s.singhania.in@gmail.com)

Mohit Law is an Associate Professor at the Department of Mechanical Engineering at the Indian Institute of Technology Kanpur, India. He received his Ph.D from the University of British Columbia, Canada. His research interests centre on understanding how and why machine tools vibrate, measuring those vibrations, and on how best to mitigate them.